Severe Mandibuloacral Dysplasia-Associated Lipodystrophy and Progeria in a Young Girl with a Novel Homozygous Arg527Cys *LMNA* Mutation

Anil K. Agarwal, Irina Kazachkova, Svetlana Ten, and Abhimanyu Garg

Division of Nutrition and Metabolic Diseases (A.K.A., A.G.), Department of Internal Medicine, Center for Human Nutrition, University of Texas Southwestern Medical Center, Dallas, Texas 75390-8537; and Infants' and Children's Hospital of Brooklyn at Maimonides (I.K., S.T.), Brooklyn, New York 11219

Context: Mandibuloacral dysplasia (MAD) is a rare autosomal recessive progeroid syndrome due to mutations in genes encoding nuclear lamina proteins, lamins A/C (*LMNA*) or prelamin A processing enzyme, and zinc metalloproteinase (*ZMPSTE24*).

Objective: The aim of the study was to investigate the underlying genetic and molecular basis of the phenotype of a 7-yr-old girl with MAD belonging to a consanguineous pedigree and with severe progeroid features and lipodystrophy.

Design and Patient: The patient developed mandibular hypoplasia during infancy and joint stiffness, skin thinning, and mottled hyperpigmentation at 15 months. Progressive clavicular hypoplasia, acroosteolysis, and severe loss of hair from the temporal and occipital areas were noticed at 3 yr. At 5 yr, cranial sutures were still open and lipodystrophy of the limbs was prominent. GH therapy from the ages of 3–7 yr did not improve the short stature. Severe joint contractures resulted in abnormal posture and decreased mobility. We studied her skin fibroblasts for nuclear morphology and immunoblotting and determined the *in vitro* effects of various pharmacological interventions on fibroblasts.

Results: *LMNA* gene sequencing revealed a homozygous missense mutation, c.1579C>T, p.Arg527Cys. Immunoblotting of skin fibroblast lysate with lamin A/C antibody revealed no prelamin A accumulation. Immunofluorescence staining of the nuclei for lamin A/C in fibroblasts revealed marked nuclear morphological abnormalities. This abnormal phenotype could not be rescued with inhibitors of farnesyl transferase, geranylgeranyl transferase, or histone deacetylase.

Conclusion: Severe progeroid features in MAD could result from *LMNA* mutation, which does not lead to accumulation of prenylated lamin A or prelamin A. **(*J Clin Endocrinol Metab* 93: 4617–4623, 2008)**

Mandibuloacral dysplasia (MAD), a rare autosomal recessive disorder, is characterized by progressive skeletal abnormalities such as delayed closure of cranial sutures, mandibular and clavicular hypoplasia, acroosteolysis of the distal phalanges, and joint contracture. Some patients show progeroid features such as bird-like facies, high-pitched voice, and ectodermal defects, such as skin atrophy, alopecia, and nail dysplasia (1–6). With the progression of time, the severity of these features increases. In addition, patients may develop two patterns of lipodystrophy—type A, characterized by partial loss of fat from extremities with excessive deposition in the face and neck; and type B, characterized by generalized loss of sc fat (1). Some patients develop hyperinsulinemia, insulin resistance, impaired glucose tolerance, diabetes mellitus and hyperlipidemia (1). Growth retardation and short adult height are commonly associated with the syndrome.

Recently, aided by careful characterization of the phenotype of lipodystrophy in MAD patients (1) and candidate gene approach, two loci have been discovered (3, 7). The first genetic locus was found to be *LMNA* gene, which by alternative

0021-972X/08/$15.00/0

Printed in U.S.A.

doi: 10.1210/jc.2008-0123 Received January 18, 2008. Accepted September 9, 2008.

First Published Online September 16, 2008

Abbreviations: FTI, Farnesyl transferase inhibitor; GGT or GGTI, geranylgeranyl transferase inhibitor; HGPS, Hutchinson-Gilford progeria syndrome; IGFBP3, IGF binding protein 3; MAD, mandibuloacral dysplasia; SNP, single nucleotide polymorphism; TSA, trichostatin A; *ZMPSTE24*, zinc metalloproteinase.

splicing encodes for nuclear lamina proteins, lamin A and C (3). The second locus is zinc metalloproteinase (*ZMPSTE24*) gene, which encodes for a protease involved in posttranslational proteolytic processing of prelamin A to its mature form, lamin A (7).

Thus far, 23 MAD patients have been reported to have *LMNA* mutations (2–6, 8, 9), but only four MAD patients have been reported with *ZMPSTE24* mutations (7, 10–12). MAD patients with *LMNA* mutations usually have normal development during the first 4 yr of life, whereas patients with *ZMPSTE24* mutations appear to have a more severe phenotype including early onset of skeletal defects such as acroosteolysis, more progeroid appearance including development of sc calcified nodules on the phalanges, and progressive glomerulopathy (10). We report an unusually severe phenotype of MAD and progeroid features in a 7-yr-old girl with a novel homozygous mutation in *LMNA* gene.

Patient and Methods

The studies were approved by the Institutional Review Boards of the University of Texas Southwestern Medical Center at Dallas, and all subjects gave a written informed consent for the studies.

Patient description

The 7-yr-old girl (MAD 2200.3) belongs to a consanguineous pedigree of German-Irish origin (Fig. 1) who developed mandibular hypoplasia during infancy resulting in crowded teeth, difficulty in swallowing and breathing, and failure to thrive. She was born full term with a birth weight of 2.55 kg (2 SD below the mean value, or −2 SD) and a length of 49 cm (−1 SD). A small and pointed nose with telangiectasia was noticed at birth. She had poor growth and weight gain. Failure to thrive was apparent by the age of 1 yr. Swallowing difficulties with frequent choking and severe snoring with obstructive apnea were frequently observed. Her dentition was normal apart from two extra lower incisors, which had to be removed. Joint stiffness, skin thinning, and mottled hyperpigmentation developed at the age of 15 months. At 2 yr of age, she developed a bird-like face with beaked nose, bulbous cheeks, and very small mouth with limited ability to open. At the initial visit at the age of 2 yr 10 months, her weight was 9.7 kg (<3 percentile), and her height was 81 cm (0.8 percentile; −3.16 SD), whereas her target height was 157.5 cm (18.3 percentile; −0.33 SD).

She was started on GH (0.4 mg/kg·wk), and her height improved to −1.48 SD within 2 yr, but she eventually developed resistance to GH secondary to GH antibody at the age of 5 yr and 2 months. Growth velocity decreased significantly thereafter, despite a higher dose of GH (0.5 mg/kg/wk). At 7 yr and 5 months of age, her height was 110 cm (<0.33 percentile, −2.72 SD), and her weight was 16.8 kg (<5th percentile). Before receiving GH therapy, her IGF-I and IGF binding protein 3 (IGFBP3) levels were 67 ng/ml (normal range, 56–144 ng/ml) and 1.7 mg/liter (normal range, 0.9–3.0 mg/liter), respectively. During GH therapy, her IGF-I levels ranged from 156 to 598 ng/ml (mean values for normal girls age 4–6 yr, 138–172 ng/ml), and IGFBP3 levels ranged from 3.0 to 6.0 mg/liter (mean values for normal girls age 4–6 yr, 2.1 to 3.0 mg/liter).

She had a senile appearance, with sparse scalp hair, thin hyperpigmented skin, paucity of body fat, and joint stiffness. Cardiac evaluation, including echocardiography, was normal. Progressive clavicular hypoplasia, acroosteolysis, and severe loss of hair from the temporal and occipital areas were noticed at 3 yr. Radiographs of the skull revealed open cranial sutures and anterior and posterior fontanelles. She had no cataracts. Her teeth were severely crowded, and several of them had already been removed. She had lipodystrophy of the gluteal region, extremities, and palmar and plantar areas (Fig. 2). Severe contractures at the joints had resulted in abnormal posture and decreased mobility. Recently, she had a rib fracture from an unnoticed trauma. Her mental development was normal. She had a high-pitched nasal voice and myopia. The skin over her entire body and extremities was thin, with easily visible veins and hyperpigmentation on the lower abdomen and buttocks. Her gait was waddling. Serum leptin level was 1.6 ng/ml (normal values from 5th to 95th percentile, 1.2 to 6.6 ng/ml), and insulin level was 1.1 μU/ml (normal value, 0–13 μU/ml).

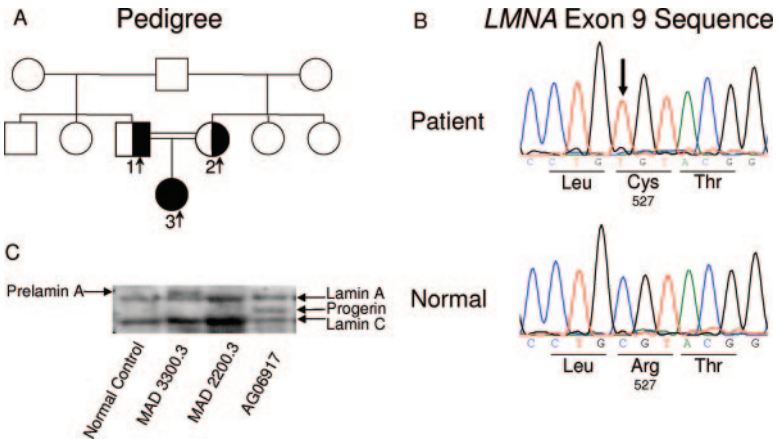

FIG. 1. MAD pedigree, *LMNA* mutation, and immunoblot from the patient's fibroblasts. A, Pedigree of the MAD family. The proband with homozygous Arg527Cys *LMNA* mutation is shown as *filled symbol*, and the parents, heterozygous for the Arg527Cys mutation, are shown as *half-filled symbols*. *Square symbols* indicate males, and *circles* indicate females. *Double horizontal lines* indicate consanguinity. B, Sequence electropherogram for mutation in exon 9 of *LMNA*. Identified mutation c.1579C>T is marked by an *arrow*, and wild-type sequence is shown below for comparison. C, Immunoblot analysis of cell lysates. Shown is a representative immunoblot of cell lysates obtained from the fibroblasts of the affected patient (MAD 2200.3) probed with amino-terminal-specific antilamin A/C antibody, N-18, showing lamin C and mature lamin A. In the affected patient, no prelamin A was identified. Patient MAD 3300.3 with ZMPSTE24 deficiency and AG06917 with HGPS (with *LMNA* G608G heterozygous mutation) were included as positive controls to show prelamin A and progerin band, respectively. Normal control subject showed lamins A and C band as well.

Anthropometry

The patient's weight and height were measured by standard procedures. Skinfold thickness measurements were carried out using Lange skinfold caliper (Cambridge Scientific Industries, Cambridge, MD) thrice on each site, and the mean value was calculated. The skinfold thickness measurements were done at the following 12 sites: chin and on the right side of body at the chest, midaxillary, abdominal, subscapular, suprailiac, biceps, triceps, forearm, hip, thigh, and calf.

Mutational analysis of the *LMNA* and *ZMPSTE24* genes

Genomic DNA was isolated from blood by using a King Fisher (Thermo Labsystems, Waltham, MA) kit according to the manufacturer's protocol. Direct sequencing of the entire coding region and the surrounding intron-exon boundaries of the *LMNA* and *ZMPSTE24* genes were conducted in the proband as reported earlier (2, 7). Primers that would amplify each exon of the *LMNA* gene from genomic DNA templates were designed from published sequence information (13). PCR was conducted as described earlier (2). For segregation analysis, only a few exons were sequenced in the parents. The PCR product was purified to re-

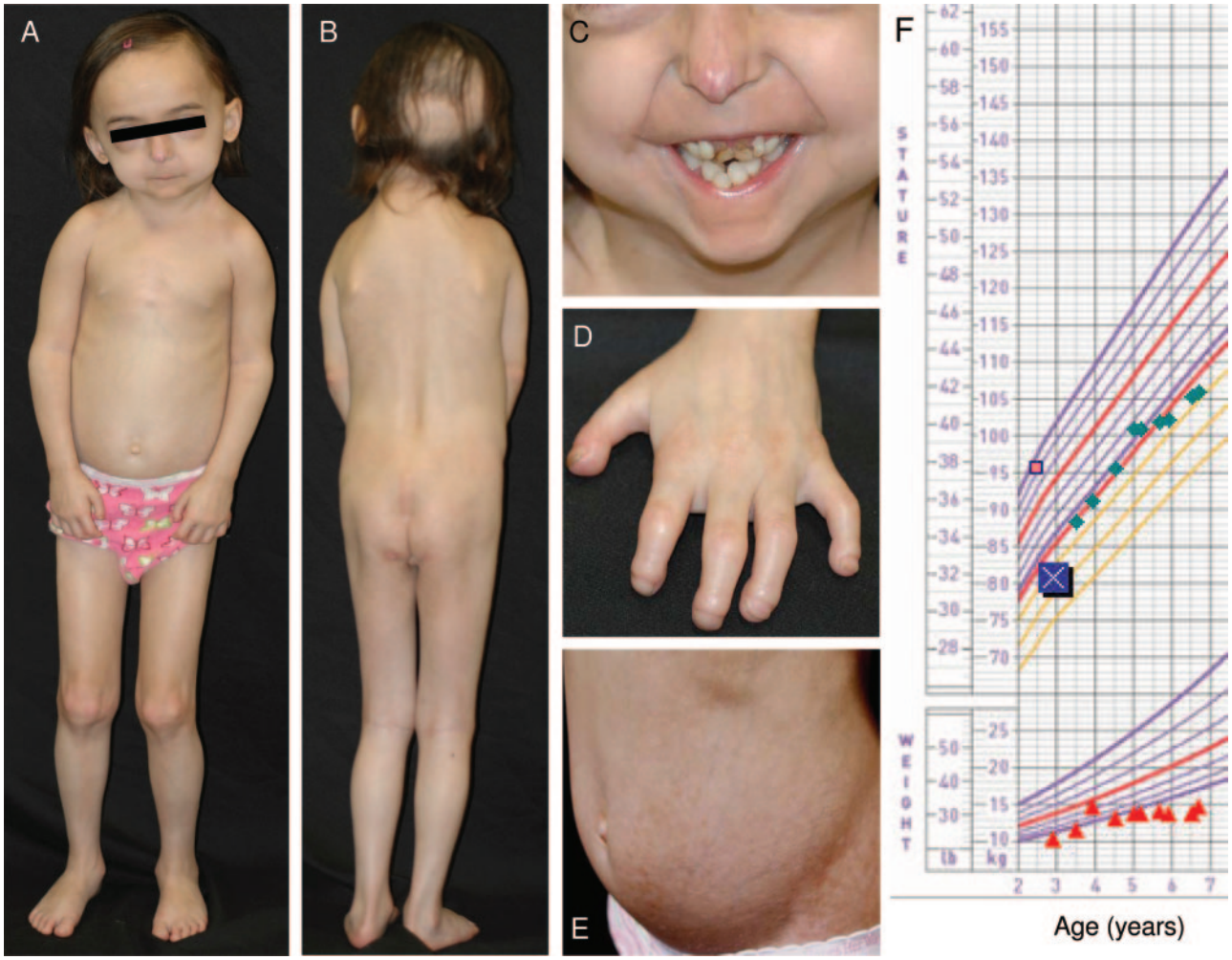

FIG. 2. Photographs of the patient at the age of 5 yr and growth chart. A, Frontal view of the total body; B, posterior view of the body; C, anterior view of the lower part of face; D, posterior view of the left hand; and E, anterior view of the abdomen. Note the characteristic faces, marked loss of scalp hair from the frontal and occipital region, mandibular hypoplasia, severe crowding of the maxillary and mandibular teeth, prominent vasculature on the tip of the nose with beaking of the nose, lipodystrophy (especially the loss of sc fat from the gluteal region), skin atrophy with mottled hyperpigmentation over the abdomen, drooping shoulders due to clavicular hypoplasia, contractures of the proximal and distal interphalangeal joints with marked acroosteolysis and finger tip rounding. F, Growth chart reveals her weight to be below the 95th percentile but an increase in linear growth with GH therapy after 3 yr of age (initial height indicated by the *symbol X*).

move primers and deoxyribonucleotide triphosphates and sequenced using ABI Prism 3100 (Perkin-Elmer Applied Biosystems, Foster City, CA).

Immunofluorescence microscopy

Immunofluorescence staining for lamin A/C was performed as described before (14). Briefly, fibroblasts (passage 2) were grown on cover slips, fixed for 20 min in methanol at −20 C, and permeabilized in 0.1% Triton X-100. The cells were incubated with antibody for lamin A, which recognizes both forms, lamin A and C (antibody H-110; Santa Cruz Biotechnology, Santa Cruz, CA) for 60 min at 37 C. The cells were washed with PBS and incubated with the secondary antibody conjugated with Alexa flour 488, green fluorescent. The DNA was stained with 4′, 6-diamidino-2-phenylindole, dihydrochloride (DAPI; Molecular Probes, Eugene, OR). After washing, the cover slips were mounted using commercial mounting medium for fluorescent microscopy, Aqua Poly/Mount (Polysciences, Inc., Warrington, PA), and images were captured using the Zeiss Axiovert 100M microscope.

Effects of pharmacological agents on nuclear morphology of fibroblasts

Preliminary experiments were performed with skin fibroblasts of healthy subjects to determine the optimum concentration of farnesyl transferase inhibitors (FTI-277 and FTI-III), geranylgeranyl transferase inhibitor (GGT-297), or a histone deacetylase inhibitor, trichostatin A (TSA), at which no toxicity was observed for the duration of the experiment. All inhibitors were from EMD Biosciences, Inc. (Gibbstown, NJ; www.vwr.com). For the studies, 10-mM stock solutions were made in dimethylsulfoxide except for FTI-III, which was dissolved in water. In our culture conditions, most cells survived for 48 h at 10-μM concentration for each of these inhibitors. All experiments were performed by incubating fibroblasts with 10-μM inhibitors for 48 h. Cells were processed for immunofluorescence microscopy as described above.

Immunoblotting

The patient's fibroblasts were lysed in lysis buffer consisting of 9 M urea, 2% Triton X-100, and protease inhibitor cocktail from Roche Diagnostic, Indianapolis, IN. The lysate was cleared by low-speed centrifugation, and the supernatant was used to determine the protein concentration by Bradford method (Bio-Rad Laboratories, Hercules, CA). A total of 100 μg of protein was resolved on 7.5% SDS-PAGE. A low-range SDS-PAGE standard was run simultaneously to determine the molecular weight of the protein (Bio-Rad Laboratories). After electrophoresis, the proteins were transferred to polyvinylidene fluoride membrane (Millipore, Billerica, MA) and blocked overnight at 4 C in 10 mM Tris buffer (pH 8.0) containing 5% nonfat milk and 0.05%

Tween-20. The blots were washed with PBS-Tween 20 and incubated with antibody to lamin A/C (N-18) at a dilution of 1:5000 for 90 min at room temperature (*sc*-6215; Santa Cruz Biotechnology), followed by incubation with secondary antibody donkey antigoat IgG-horseradish peroxidase at a dilution of 1:10,000 (*sc*-2033, Santa Cruz Biotechnology). The blots were washed and developed with chemiluminescent horseradish peroxidase substrate from Millipore to visualize the immunoreactive protein. Images were captured using Alpha Innotech imaging system (Alpha Innotech Corp., San Leandro, CA). Cell lysates from two positive control subjects, one with ZMPSTE24 deficiency (showing prelamin A) and another with Hutchinson-Gilford progeria syndrome (HGPS; showing progerin), and from a normal control subject were also run simultaneously on the gel.

Biochemical analyses

Plasma insulin and leptin levels were determined by RIAs using commercial kits (Linco Research, Inc., St. Charles, MO). Serum lipoproteins, glucose, and chemistry were measured by the Beckman CX9ALX chemistry analyzer (Beckman Instruments, Fullerton, CA).

Results

The skinfold thickness measurements confirmed the presence of type A or partial lipodystrophy noted on physical examination. Her skinfold thickness at the peripheral sites, such as the triceps, thigh, and calf, was below the 10th percentile value of the matched controls (Fig. 3). Even some truncal skinfolds, such as the axillary, subscapular, and suprailiac, were below the 10th percentile; however, the chest and abdominal skinfold thicknesses were close to 50th percentile. Metabolic assessment revealed normal fasting glucose (79 mg/dl) concentration. Serum total cholesterol and low-density lipoprotein cholesterol were in the normal range. At the age of 2 yr and 10 months, her serum triglyceride concentration was 127 mg/dl, and high-density lipoprotein cholesterol was 37 mg/dl.

The mutational analysis of the coding region and the adjacent splice sites of the *LMNA* gene revealed a homozygous p.Arg527Cys (c.1579 C>T) mutation in exon 9 in the patient (Fig. 1B). No mutations were noted in the *ZMPSTE24* gene. We determined haplotypes associated with the c.1579 C>T *LMNA* mutation using intragenic single nucleotide polymorphisms (SNPs) extending 2.5 kb around the site of mutation. The affected subject from our pedigree was homozygous for all the intragenic SNPs. The haplotype was CC-TT-CC-AA-TT-CC-CC for the following SNPs: 51C>T, 861 T>C, IVS5-7 C>G, IVS6 + 16G>A, 1338T>C, IVS8 + 44C>T, and 1698C>T. This haplotype was different than those reported earlier (2, 3).

Both parents were heterozygous for the p.Arg527Cys *LMNA* mutation and were healthy, without any skeletal anomalies or progeroid features. The mother, who was 27 yr old, had no diabetes, hypertriglyceridemia, or hypertension. She had normal skinfold thickness, and her serum chemistry including lipid profile was normal. The father was 33 yr old and had hyperlipidemia, hypertension, and a renal infarct at age 32. He had mildly elevated low-density lipoprotein cholesterol of 4.32 mmol/liter but had normal high-density lipoprotein cholesterol of 1.05 mmol/liter and triglyceride levels of 1.50 mmol/liter. He also had impaired fasting glucose with levels of 6.61 mmol/liter.

Immunoblots from the fibroblasts of our patient and the normal control subject showed the presence of lamins A and C without any additional higher molecular weight band, which corresponds to prelamin A or an intermediate molecular weight band corresponding to progerin (Fig. 1C).

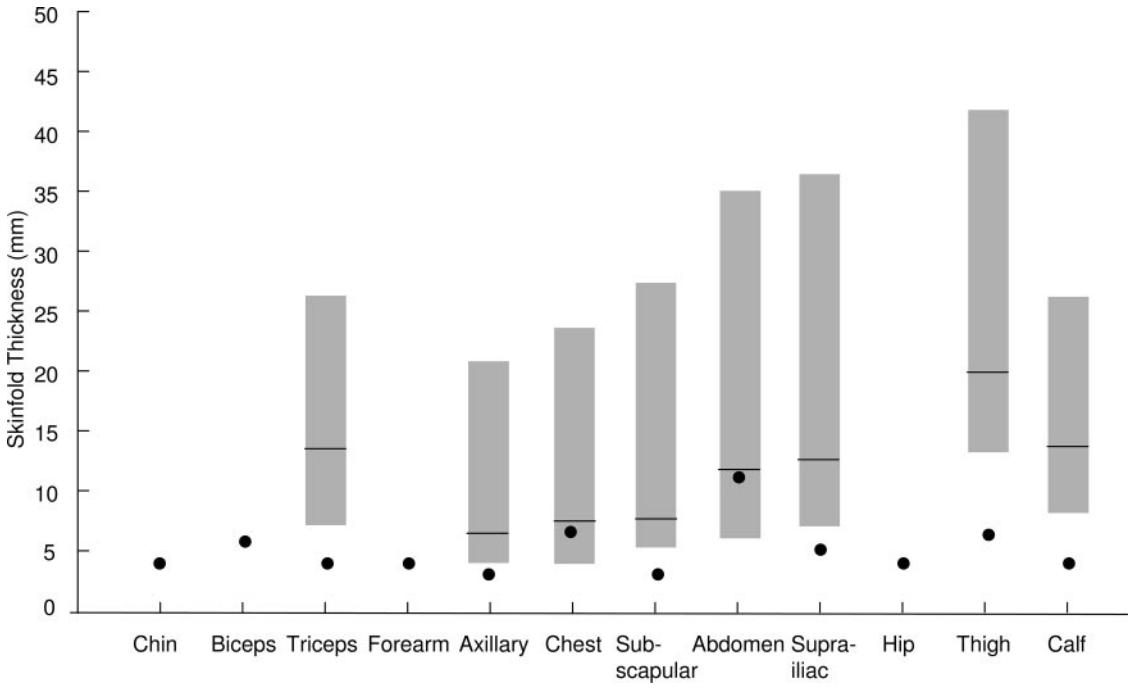

FIG. 3. Skinfold thickness at various anatomic sites of our patient. Data from our patient are shown as *filled circles*. The *shaded bars* represent the median, 10th and 90th percentile values of skinfold thickness for normal 4- to 10-yr-old girls. [The data were collected on 106 females. The mean body mass index was 19.1 kg/m^2 (range, 12.8 to 34 kg/m^2). There were 49 White girls from Vermont and 19 White and 38 Black girls from Alabama (27). Courtesy of M. I. Goran.] Clearly, her thigh, calf, triceps, suprailiac, and subscapular skinfold thickness was well below the 10th percentile of normal girls, suggestive of partial lipodystrophy.

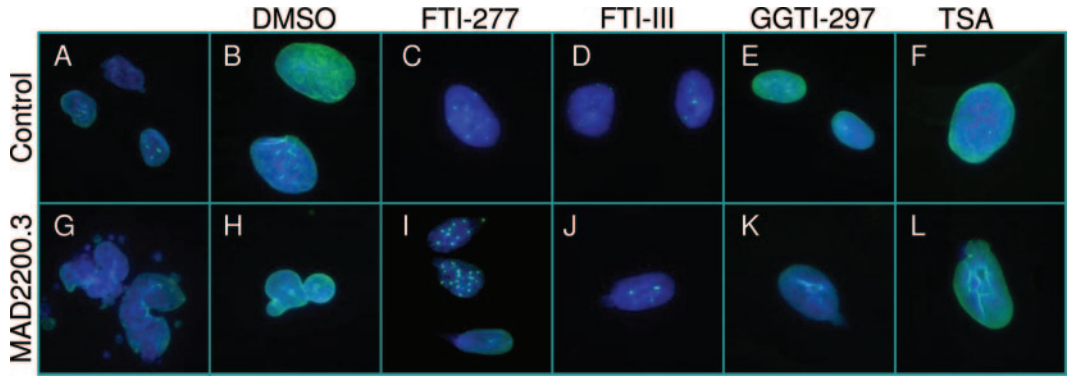

FIG. 4. Nuclear morphology of skin fibroblasts and response to various pharmacological agents. Indirect immunofluorescence microscopy using lamin A/C antibody (H-110) in fibroblasts obtained from a control subject and the patient, MAD 2200.3. A and B, Control cells in culture medium without and with dimethylsulfoxide (DMSO). C—F, Morphology after incubation of the cells for 48 h with 10 μM FTI-277 or FTI-III, GGT-297, or a histone deacetylase inhibitor, TSA, respectively. G and H, Fibroblasts from patient MAD 2200.3 showed misshapen nuclei with bilobed nuclei or nuclear blebs. These nuclear abnormalities did not affect the localization of lamin A to the periphery of the nucleus. I—L, Incubation of the cells with FTI-277, FTI-III, GGT-297 or TSA, respectively, did not correct these nuclear abnormalities. Note the aggregation of lamin A/C in the fibroblast nuclei from both the control and the patient incubated with FTIs (panels C, I).

Microscopic examination of nuclei from skin fibroblasts of the affected subject showed one or two misshapen nuclei in a field of 10–12 nuclei, such as bilobed nuclei or nuclear blebs, which were not seen in fibroblasts from the normal control (Fig. 4). These nuclear abnormalities did not affect the localization of lamin A. Incubation of these cells with FTI-277, FTI-III, or GGT-297 could not rescue these nuclear abnormalities. Interestingly, both in control fibroblasts and those from the patient, FTIs resulted in some aggregation of lamin A/C staining. Finally, addition of TSA also did not improve nuclear morphological abnormalities. However, with TSA, no lamin A/C aggregates were observed.

Discussion

We report a young girl with a severe phenotype of MAD and progeria associated with a novel homozygous *LMNA* missense mutation. So far, mutations in *LMNA* gene have been reported in 23 patients with MAD, which include homozygous Arg527His mutation in six Italian and two Hispanic pedigrees, homozygous Ala529Val mutation in two Turkish pedigrees, homozygous Ala529Thr mutation in a Japanese woman, homozygous Lys542Asn mutation in an Indian pedigree, and compound heterozygous Arg471Cys/Arg527Cys and Arg527His/Val440Met mutations in two Caucasian patients (1–6, 8, 9, 15). The phenotype of our patient is more severe than those reported previously in MAD patients with homozygous Arg527His, Ala529Val, or Ala529Thr *LMNA* mutations (2, 3, 6, 8). The onset of acroosteolysis occurred in patients with Arg527His or Ala529Val *LMNA* mutations at about 4 yr of age. Alopecia has not been reported previously in patients with MAD at such a young age as 3 yr. We also did not observe hair loss in three female (ages 16, 20, and 21 yr) and two male (ages 12 and 18 yr) patients with Arg527His or Ala529Val mutations who were reported earlier (1, 2, 5). Novelli *et al.* (3) did report subtotal alopecia of scalp but only in male patients with Arg527His mutation; the age of onset of alopecia, however, was not reported. Furthermore, lipodystrophy in MAD patients has been reported with onset at the time of puberty. Our patient had onset of lipodystrophy much earlier. She had poor linear growth and also developed severe contractures of the joints resulting in reduced mobility. All these clinical features suggest an unusually severe phenotype associated with Arg527Cys homozygous mutation. Interestingly, heterozygous Arg527Cys mutation has also been associated with MAD phenotype, although in association with heterozygous Arg471Cys mutation (15). However, only limited clinical information is available about this patient from the Coriell repository. The patient was a 28-yr-old female with severe osteoporosis and multiple fractures who had normal sexual development with onset of acroosteolysis at the age of 2 yr. She was reported to have developed alopecia at the age of 28 yr.

Previously, affected patients from an Indian pedigree were reported to have severe progeria features suggestive of HGPS (alopecia, lack of eyebrows and eyelashes, and absent or impaired sexual maturation) in association with a homozygous Lys542Asn mutation (4). Two of them died at ages 10 and 16 yr. However, because all affected patients had mandibular and clavicular hypoplasia and acroosteolysis and because the pattern of inheritance was autosomal recessive, we think that they had MAD. Severity of clinical features of our patient does compare to those observed in affected subjects from the Indian pedigree.

Recently, an in-depth phenotypic evaluation of 15 children with HGPS with G608G *LMNA* mutation has helped to clarify differences in clinical features between MAD and HGPS (16). Alopecia and generalized lipodystrophy were seen in all patients with HGPS. Although acroosteolysis, clavicular resorption, and coxa valga were also seen in all patients with HGPS, compared with patients with MAD, they had only mild acroosteolysis (16). The mean age of death in HGPS patients is 12.6 yr, usually due to myocardial infarction, intracranial bleeding, or stroke (17). These vascular complications so far have not been reported in patients with MAD. Circumoral cyanosis also seems to be a peculiar feature in HGPS patients (16). Both types of patients have sclerodermatous skin, joint contractures, hypo- and hyperpigmented skin lesions, and short stature.

Our patient developed severe short stature (-3.1 SD) by the age of 2½ yr. Delayed bone age and low levels of serum IGF-I and

IGFBP3 were suggestive of GH deficiency, although the decrease in IGF-I did not correlate with the severity of growth retardation. Because a GH stimulation test was not done, it is impossible to conclude whether her early growth retardation was the result of the severity of the expressed MAD syndrome or a coincident GH deficiency. She responded well to exogenous GH therapy initially. However, growth velocity decreased significantly after she developed GH antibody, despite receiving a higher dose of GH. Thus, it remains unclear whether GH therapy should be considered to increase linear growth in such patients with MAD.

The lamin A/C polypeptide from amino acids 470 to 545 has been crystallized and shown to assume an Ig domain (18). We have previously modeled the substitution of Arg 527 to His, which showed disruption of the salt bridge between Arg 527 and Glu at position 537 (5). Similar salt bridge disruption was also observed when Arg 527 was substituted with Cys. Thus it remains unclear why substitution of Arg 527 with His is associated with a milder phenotype than its substitution with cysteine. The molecular mechanisms explaining wide differences in the phenotypic manifestations in patients with MAD associated with different *LMNA* mutations remain to be elucidated.

Our patient's skin fibroblasts revealed more marked nuclear morphological abnormalities than reported previously in patients with either homozygous Arg527His or Ala529Val mutations (3, 5, 19). However, the immunoblot analysis of fibroblast cell lysates showed no evidence of accumulation of prelamin A. This is in contrast to previous reports (19, 20) where accumulation of prelamin A in fibroblast cell lysates from patients with MAD was observed.

Although we were unable to detect any prelamin A in the fibroblast cell lysates, we wished to study the effects of FTIs on nuclear morphology because of the possibility that the levels of abnormal prelamin A in our patient may be so low that it is undetectable on our immunoblot. Another possibility is that if the mutant lamin A cannot undergo farnesylation, it may be geranylgeranylated by geranylgeranyl transferase (21). Therefore, we also incubated the cells with inhibitors of geranylgeranyl transferase to explore that possibility. Our results do not reveal any significant effects of FTIs or GGTI on rescuing the abnormalities in nuclear morphology in our patient's fibroblast cells. The rationale for TSA treatment, a histone deacetylase inhibitor, was that the mutation Arg527Cys might disrupt the assembly of nucleosomes that are dependent on histone deacetylation. Exposing fibroblasts to TSA again failed to show any measurable improvements in the nuclear morphology. Whether various combinations of FTIs, GGTIs, and TSA will improve nuclear function in patients with MAD remains to be determined.

These results are in contrast to the allelic progeroid disorder, HGPS, in which progerin (a truncated form of farnesylated prelamin A) accumulates, where FTIs have been shown to improve nuclear morphological abnormalities, but only in about 50% of the cells (22, 23). FTIs and TSA have also been reported to rescue nuclear heterochromatin organization in fibroblasts from HGPS patients (24). However, we did not study the nuclear heterochromatin organization in our patient's fibroblasts. Nonetheless, our data suggest that progeroid features in our patient with MAD may not be related to the accumulation of farnesylated prelamin A or other mutant lamin A forms, but they could be due to other biochemical mechanisms.

The cellular senescence occurs via a variety of molecular processes. Accumulation of prenylated prelamin A is one of them. Nevertheless, other mechanisms may also operate at the cellular level that may result in less severe phenotype. More recent observations have led to the hypothesis that lamins are involved in membrane support, nuclear pore arrangement, nuclear envelope assembly, and chromatin organization and may thus control diverse functions such as DNA synthesis, gene expression, and apoptosis (20, 25, 26). It is likely that in our patient, abnormal mutant lamin A may directly disrupt these vital processes, resulting in cellular toxicity.

Acknowledgments

Address all correspondence and requests for reprints to: Abhimanyu Garg, M.D., Division of Nutrition and Metabolic Diseases, University of Texas Southwestern Medical Center at Dallas, 5323 Harry Hines Boulevard, Dallas, Texas 75390-8537. E-mail: abhimanyu.garg@utsouthwestern.edu.

This work was supported by National Institutes of Health Grants R01-DK54387 and M01-RR00633, and by the Southwest Medical Foundation.

Disclosure Statement: All authors have nothing to declare.

References

1. **Simha V, Garg A** 2002 Body fat distribution and metabolic derangements in patients with familial partial lipodystrophy associated with mandibuloacral dysplasia. J Clin Endocrinol Metab 87:776–785
2. **Simha V, Agarwal AK, Oral EA, Fryns JP, Garg A** 2003 Genetic and phenotypic heterogeneity in patients with mandibuloacral dysplasia-associated lipodystrophy. J Clin Endocrinol Metab 88:2821–2824
3. **Novelli G, Muchir A, Sangiuolo F, Helbling-Leclerc A, D'Apice MR, Massart C, Capon F, Sbraccia P, Federici M, Lauro R, Tudisco C, Pallotta R, Scarano G, Dallapiccola B, Merlini L, Bonne G** 2002 Mandibuloacral dysplasia is caused by a mutation in *LMNA*-encoding lamin A/C. Am J Hum Genet 71:426–431
4. **Plasilova M, Chattopadhyay C, Pal P, Schaub NA, Buechner SA, Mueller H, Miny P, Ghosh A, Heinimann K** 2004 Homozygous missense mutation in the lamin A/C gene causes autosomal recessive Hutchinson-Gilford progeria syndrome. J Med Genet 41:609–614
5. **Garg A, Cogulu O, Ozkinay F, Onay H, Agarwal AK** 2005 A novel homozygous Ala529Val LMNA mutation in Turkish patients with mandibuloacral dysplasia. J Clin Endocrinol Metab 90:5259–5264
6. **Shen JJ, Brown CA, Lupski JR, Potocki L** 2003 Mandibuloacral dysplasia caused by homozygosity for the R527H mutation in lamin A/C. J Med Genet 40:854–857
7. **Agarwal AK, Fryns JP, Auchus RJ, Garg A** 2003 Zinc metalloproteinase, ZMPSTE24, is mutated in mandibuloacral dysplasia. Hum Mol Genet 12:1995–2001
8. **Kosho T, Takahashi J, Momose T, Nakamura A, Sakurai A, Wada T, Yoshida K, Wakui K, Suzuki T, Kasuga K, Nishimura G, Kato H, Fukushima Y** 2007 Mandibuloacral dysplasia and a novel LMNA mutation in a woman with severe progressive skeletal changes. Am J Med Genet A 143:2598–2603
9. **Lombardi F, Gullotta F, Columbaro M, Filareto A, D'Adamo M, Vielle A, Guglielmi V, Nardone AM, Azzolini V, Grosso E, Lattanzi G, D'Apice MR, Masala S, Maraldi NM, Sbraccia P, Novelli G** 2007 Compound heterozygosity for mutations in LMNA in a patient with a myopathic and lipodystrophic mandibuloacral dysplasia type A phenotype. J Clin Endocrinol Metab 92:4467–4471
10. **Agarwal AK, Zhou XJ, Hall RK, Nicholls K, Bankier A, Van Esch H, Fryns J-P, Garg A** 2006 Focal segmental glomerulosclerosis in patients with mandibu-

loacral dysplasia due to zinc metalloproteinase deficiency. J Invest Med 54: 208–213
11. **Denecke J, Brune T, Feldhaus T, Robenek H, Kranz C, Auchus RJ, Agarwal AK, Marquardt T** 2006 A homozygous ZMPSTE24 null mutation in combination with a heterozygous mutation in the LMNA gene causes Hutchinson Gilford Progeria Syndrome (HGPS): insights into the pathophysiology of HGPS. Hum Mutat 27:524–531
12. **Shackleton S, Smallwood DT, Clayton P, Wilson LC, Agarwal AK, Garg A, Trembath RC** 2005 Compound heterozygous ZMPSTE24 mutations reduce prelamin A processing and result in a severe progeroid phenotype. J Med Genet 42:e36
13. **Lin F, Worman HJ** 1993 Structural organization of the human gene encoding nuclear lamin A and nuclear lamin C. J Biol Chem 268:16321–16326
14. **Jacob KN, Baptista F, dos Santos HG, Oshima J, Agarwal AK, Garg A** 2005 Phenotypic heterogeneity in body fat distribution in patients with atypical Werner's syndrome due to heterozygous Arg133Leu lamin A/C mutation. J Clin Endocrinol Metab 90:6699–6706
15. **Cao H, Hegele RA** 2003 LMNA is mutated in Hutchinson-Gilford progeria (MIM 176670) but not in Wiedemann-Rautenstrauch progeroid syndrome (MIM 264090). J Hum Genet 48:271–274
16. **Merideth MA, Gordon LB, Clauss S, Sachdev V, Smith AC, Perry MB, Brewer CC, Zalewski C, Kim HJ, Solomon B, Brooks BP, Gerber LH, Turner ML, Domingo DL, Hart TC, Graf J, Reynolds JC, Gropman A, Yanovski JA, Gerhard-Herman M, Collins FS, Nabel EG, Cannon 3rd RO, Gahl WA, Introne WJ** 2008 Phenotype and course of Hutchinson-Gilford progeria syndrome. N Engl J Med 358:592–604
17. **Hennekam RC** 2006 Hutchinson-Gilford progeria syndrome: review of the phenotype. Am J Med Genet A 140:2603–2624
18. **Dhe-Paganon S, Werner ED, Chi YI, Shoelson SE** 2002 Structure of the globular tail of nuclear lamin. J Biol Chem 277:17381–17384
19. **Filesi I, Gullotta F, Lattanzi G, D'Apice MR, Capanni C, Nardone AM, Columbaro M, Scarano G, Mattioli E, Sabatelli P, Maraldi NM, Biocca S, Novelli G** 2005 Alterations of nuclear envelope and chromatin organization in mandibuloacral dysplasia, a rare form of laminopathy. Physiol Genomics 23: 150–158
20. **Meaburn KJ, Cabuy E, Bonne G, Levy N, Morris GE, Novelli G, Kill IR, Bridger JM** 2007 Primary laminopathy fibroblasts display altered genome organization and apoptosis. Aging Cell 6:139–153
21. **Varela I, Pereira S, Ugalde AP, Navarro CL, Suárez MF, Cau P, Cadiñanos J, Osorio FG, Foray N, Cobo J, de Carlos F, Lévy N, Freije JMP, López-Otín** C 2008 Combined treatment with statins and aminobisphosphonates extends longevity in a mouse model of human premature aging. Nat Med 14:767–772
22. **Glynn MW, Glover TW** 2005 Incomplete processing of mutant lamin A in Hutchinson-Gilford progeria leads to nuclear abnormalities, which are reversed by farnesyltransferase inhibition. Hum Mol Genet 14:2959–2969
23. **Capell BC, Erdos MR, Madigan JP, Fiordalisi JJ, Varga R, Conneely KN, Gordon LB, Der CJ, Cox AD, Collins FS** 2005 Inhibiting farnesylation of progerin prevents the characteristic nuclear blebbing of Hutchinson-Gilford progeria syndrome. Proc Natl Acad Sci USA 102:12879–12884
24. **Columbaro M, Capanni C, Mattioli E, Novelli G, Parnaik VK, Squarzoni S, Maraldi NM, Lattanzi G** 2005 Rescue of heterochromatin organization in Hutchinson-Gilford progeria by drug treatment. Cell Mol Life Sci 62:2669–2678
25. **Pan Y, Garg A, Agarwal AK** 2007 Mislocalization of prelamin A Tyr646Phe mutant to the nuclear pore complex in human embryonic kidney 293 cells. Biochem Biophys Res Comm 355:78–84
26. **Nitta RT, Jameson SA, Kudlow BA, Conlan LA, Kennedy BK** 2006 Stabilization of the retinoblastoma protein by A-type nuclear lamins is required for INK4A-mediated cell cycle arrest. Mol Cell Biol 26:5360–5372
27. **Dezenberg CV, Nagy TR, Gower BA, Johnson R, Goran MI** 1999 Predicting body composition from anthropometry in pre-adolescent children. Int J Obes Relat Metab Disord 23:253–259